



Analysis and Experimentation of Soft Switched Interleaved Boost Converter for Photovoltaic Applications

N. Subramanian, P. Prasanth, R. Srinivasan, R. R. Subhesh, R. Seyezhai*

Department of EEE, SSN College of Engineering, Chennai, India

PAPER INFO

Paper history:

Received 17 June 2015
Received in revised form 01 July 2015
Accepted 03 September 2015

Keywords:

Soft Switching
Auxiliary Tank
Power Loss Reduction
Photovoltaic

ABSTRACT

Conventional energy sources are fast depleting due to poor conservation practises and excessive usage while the world's energy demands are growing by minute. Additionally, the cost of producing conventional energy is rising also leading to an increase in harmful environmental pollution. Hence, there is a need to look at alternative energy sources such as sun, water and wind. Photovoltaic (PV) is a very promising option as it uses energy from naturally available sunlight distributed throughout the Earth which is not only pollution free but also abundant and recyclable in nature. Among the different DC-DC converters proposed in literature, interleaved boost converter is best suited for PV and other high power density applications. Conventional interleaved boost converters experience switching losses and switching stresses during turn-on and turn-off periods due to hard switching. In order to eliminate the power loss in the converter devices, soft switched interleaved boost converter (IBC) is proposed in this paper. Soft switching is achieved with the use of an LC resonant tank circuit. The tank circuit is responsible for zero voltage switching (ZVS) and zero current switching (ZCS), eliminating the power loss in the switches appreciably. Since photovoltaic source is used as the input to the converter, a maximum power point tracking (MPPT) algorithm is implemented to extract maximum available power from the PV panel. Furthermore, the device losses, ripple and current sharing based on input and output characteristics are recorded and examined. Simulation study of the design is carried out using MATLAB/SIMULINK software. A hardware prototype with PV module is developed to validate the simulation results.

doi: 10.5829/idosi.ije.2015.28.10a.10

1. INTRODUCTION

Interleaving in the boost converter effectively reduces the ripple as a function of duty cycle. Interleaving of boost converters is done to minimize the input current ripple, output voltage ripple, reduce the passive component size, improve the transient response and increase the power level making them ideal for high power density applications. In boost converters, due to fast turn-on and turn-off of the switches, there is considerable power loss in the devices. This method of switching the devices is called hard switching. These losses are highly responsible for lowering the converter performance. Hence, soft switching technique is used where the voltage and current through the switches are

forced to zero before turning on and turning off the devices respectively. It is known as zero voltage switching (ZVS) and zero current switching (ZCS). The ZVS and ZCS are achieved using an LC resonant tank in the interleaved boost converter. The soft switching technique [1-4] helps in eliminating the switching losses and stresses to a large extent and is found to be more efficient when compared to the hard switching technique in conventional boost converters.

Photovoltaic system design has two parameters for consideration: solar irradiation and temperature. It is required to supply a constant output voltage to the load irrespective of the variation in the temperature and solar irradiation levels. Since the relationship between voltage and current in a PV array is non-linear, it is difficult to extract maximum power from the solar panel. As a result, it is necessary to employ a maximum

* Corresponding Author's Email: seyezhair@ssn.edu.in (R. Seyezhai)

power point tracking algorithm to extract maximum power at any given point from a low voltage PV source which can then be used in supplying power. The low voltage PV source is coupled with the soft switched interleaved boost converter that encounters low levels of switching losses and switching stresses in the converter circuit. As a result of coupling, the ripple contents at the input current and output voltage are reduced maximising the system efficiency. This is accomplished by adopting a soft switched interleaved boost converter topology. The input current is shared equally between the switches. The circuit can drive heavy loads with high levels of efficiency due to impedance matching achieved by energy storing elements (resonant tank and variable output capacitor). Better switch timing for ZVS and ZCS is also obtained using bypass networks [5]. The clamped diode acts as a bypass path reducing the conduction losses. Coupling capacity between auxiliary unit and main switches reduces the voltage stress of the switches during switching operations.

The paper in sections begins with outlining the phases of operation of soft switched IBC circuit with explaining how each phase works [6]. The next section highlights the design considerations of IBC. The subsequent section covers interfacing of IBC with PV module, whose validation is done through the simulation results of soft switched IBC with PV module and MPPT and PV panel characteristics.

The section that follows, details the simulation waveforms of soft switched IBC highlighting the advantages of soft switching over conventional hard switching techniques. The ripple values, switching device losses and IBC efficiency are calculated to amply prove that the soft switched IBC using an auxiliary resonant tank circuit is indeed an ideal fit for PV applications. Finally, to validate the simulation results a hardware prototype is implemented.

2. SOFT SWITCHED IBC CIRCUIT

The circuit of soft switched IBC is shown in Figure 1. The circuit consists of two main switches (S_{S1} and S_{S2}), an auxiliary switch S_{ax} , three diode rectifiers (D_S , D_{r1} , D_{r2}) and two clamped diodes (D_r and D_c). The circuit has two boost inductors B_{L1} and B_{L2} as in the basic IBC topology and soft switching is achieved using a resonant tank comprised of a resonant capacitor C_{rc} and resonant inductor L_{rc} which are responsible for ZVS and ZCS function [7, 8].

2.1. Operation of Soft Switched IBC The IBC is operated with a duty cycle of 40%. There are eighteen operational phases in one complete cycle.

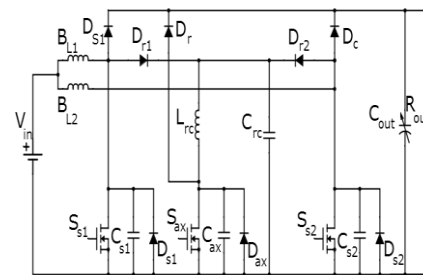


Figure 1. Schematic of two-phase IBC

Out of the eighteen phases, nine are related to main switch S_{S1} and the others to main switch S_{S2} . The output is equal for both switches due to the symmetrical nature of the interleaving circuit [2].

The driving signals for the main switches and the auxiliary switch are shown in Figure 2. The various current waveforms and voltage waveforms during the different phases are also shown in Figure 3.

The modes of operation are divided into nine modes and in mode-1, the control of switches is excited by pulse which is meant to turn off the switches S_{S1} and S_{S2} . Hence, the parasitic capacitance of the two main switches C_{S1} and C_{S2} gets charged. The voltage across the parasitic capacitors C_{S1} and C_{S2} of the main switches and resonant capacitor C_{rc} are all equal to the output voltage i.e., $V_{S1}=V_{S2}=V_{rc}=V_0$ in the previous phase. The resonant inductor current I_{Lrc} linearly ramps up until it reaches I_{in} at $t=t_1$. During t_1-t_2 , the resonant inductor keeps on charging and continues to increase to the peak value during which the main switch voltages V_{S1} and V_{S2} decrease to zero, because of resonance among C_{S1} , C_{S2} , C_{rc} , L_{rc} [3]. Then, the body diodes D_{S1} and D_{S2} of switches S_{S1} and S_{S2} , respectively, can be turned ON. In the interval, t_2-t_3 , the main switch voltage V_{S1} decreases to zero. As a result the body diode D_{S1} of switch S_{S1} is turned ON at t_2 . At this time, the main switch can achieve ZVS.

During t_3-t_4 , the auxiliary switch S_{ax} is turned OFF and the clamped diode D_r is turned ON. During this time interval, the energy stored in the resonant inductor L_{rc} is transferred to the output load. The resonant inductor current I_{Lrc} decreases to zero and the clamped diode D_r is turned OFF at t_4 . In the interval t_4-t_5 , the clamped diode D_r is turned OFF. The energy of the boost inductor L_2 is transferred to C_{rc} and C_{S2} and the energy stored in the parasitic capacitor C_{ax} of the auxiliary switch is transferred to the resonant inductor L_{rc} and the resonant capacitor C_{rc} at this time.

During t_6-t_7 , the clamped diode D_r is turned ON. The energy stored in the resonant inductor L_{rc} is transferred to the output load by the clamped diode D_r . At t_7 , the clamped diode D_r is turned OFF because the auxiliary switch S_r is turned ON.

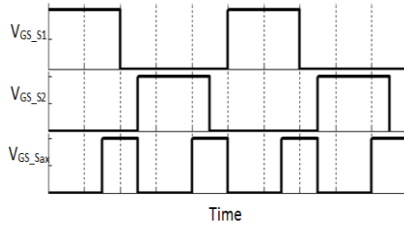


Figure 2. Driving signal for switches

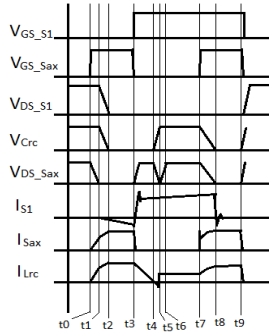


Figure 3. Switching phases

During the time interval t_7 - t_8 , the resonant inductor current continues to increase to the peak value and the main switch voltage V_{S2} decreases to zero because of resonance among C_{S2} , C_{rc} and L_{rc} . At $t=t_8$, the body diode D_{S2} of switch S_{S2} is turned ON. In this phase, the resonant inductor current I_{Lrc} equals the inductor current I_{L2} . This state is called critical state where the rectified input to the switches is zero. So, the switch S_{S1} tends to achieve ZCS. As a result the switch S_{S1} is turned OFF at the end of t_9 . The energy stored in the resonant inductor L_{rc} is transferred to the output load by the clamped diode D_r .

2. 2. Design of IBC The output voltage of IBC can be obtained from the following relation:

$$V_o = \frac{V_{in}}{1-D} \quad (1)$$

where V_o is the output voltage, V_{in} is the input voltage and D is the duty cycle.

The boost inductors L_1 and L_2 are calculated based on parameters such as switching frequency f_s , input and output voltage, inductor current ripple ΔI_L .

$$L_1 = L_2 = L = \frac{V_{in} * (V_o - V_{in})}{\Delta I_L * f_s * V_o} \quad (2)$$

ΔI_L is calculated as:

$$\Delta I_L = (0.2) * I_{out} * \frac{V_o}{V_{in}} \quad (3)$$

The value I_{outmax} is calculated as:

$$I_{outmax} = \frac{P_o}{V_o} \quad (4)$$

where P_o is the output power of IBC.

The output capacitance is calculated as:

$$C_o = \frac{I_{outmax} * D}{f_s * \Delta V_o} \quad (5)$$

where ΔV_o is the output voltage ripple and it is taken as 5% of the output voltage V_o . The resonant frequency f_r is:

$$f_r = \frac{1}{2\pi\sqrt{L_{rc}C_{rc}}} \quad (6)$$

By fixing the value of f_r and C_{rc} , the value of L_{rc} is calculated as:

$$L_{rc} = \frac{1}{f_r^2 * 4 * \pi^2 * C_{rc}} \quad (7)$$

Using the above design equations [9], the simulation parameters for IBC is calculated as shown in Table 1.

3. INTERFACE OF IBC WITH PV MODULE

In order to use the IBC for photovoltaic applications, a PV module is used to supply power to the IBC [10]. The relationship between current and voltage in a PV panel is shown in Figure 4.

TABLE 1. Simulation parameters for IBC

Parameter	Value
Input voltage (V_{in})	21.16V
Duty cycle(D)	40%
Switching frequency(f_s)	25kHz
Inductors (L_1 and L_2)	376.18 μ H
Resonant frequency (f_r)	50kHz
Resonant inductor (L_{rc})	6.67 μ H
Resonant capacitor (C_{rc})	1.5 μ F
Output capacitor (C_o)	25 μ F
Output resistor (R_o)	13.05 Ω

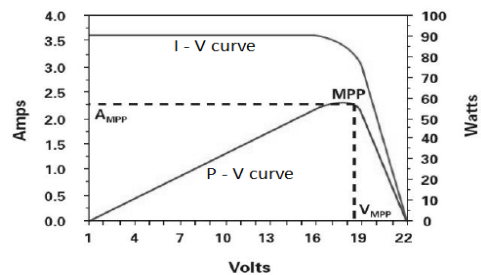


Figure 4. I-V and P-V curve characteristics for a sample panel

From the figure, it can be found that the relationship between current and voltage is non-linear and it is difficult to draw the maximum power from the panel. Hence, a maximum power point tracking (MPPT) algorithm is used to draw maximum power from the panel [11]. According to maximum power transfer theorem, when the load impedance matches with the source impedance, maximum power can be transferred from the source to the load. Hence the problem of tracking the maximum power point reduces to an impedance matching problem. There are many types of algorithm to track the maximum power. The algorithm used here is the Perturb and Observe algorithm [2]. It is the simplest algorithm of all. The algorithm is shown in Figure 5. The complete block diagram is shown in Figure 6. The specification of the PV panel is shown in Table 2.

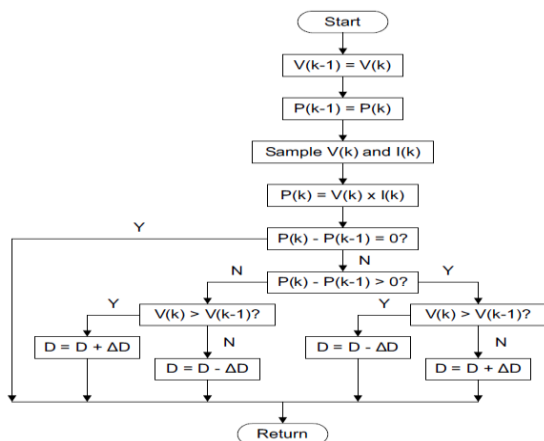


Figure 5. Flowchart of Perturb & Observe algorithm

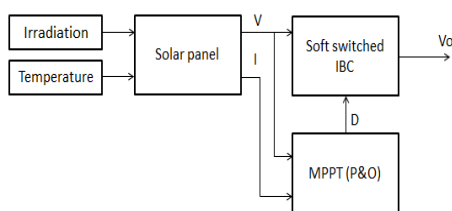


Figure 6. Block diagram of soft switched IBC with PV and MPPT

TABLE 2. Simulation parameters for PV

Parameter	Value
Open circuit voltage (V_{OC})	21.16V
Short circuit current (I_{SC})	5.87A
Voltage at maximum power point (V_{MPP})	17.53V
Current at maximum power point (I_{MPP})	5.43A
Maximum power	95.187W

4 SIMULATION OF SOFT SWITCHED IBC WITH PV MODULE AND MPPT

4. 1. Simulation Results of PV Panel Characteristics

Using the simulation parameters as in Table 2, the simulation results of the PV panel characteristics is shown in Figures 7 and 8 [1]. From the above curves, it can be seen that the maximum attained power is 95W at a voltage of 21V.

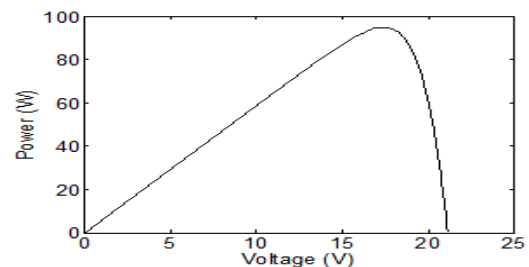


Figure 7. P-V curve of panel

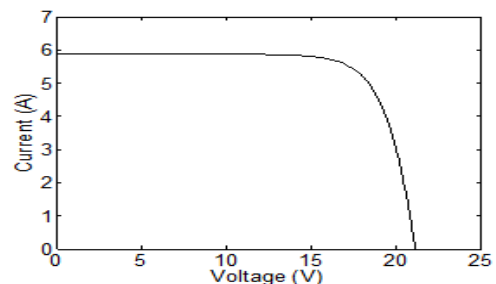


Figure 8. I-V curve of panel

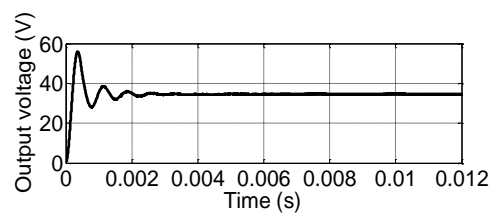


Figure 9. Output voltage waveform of the IBC

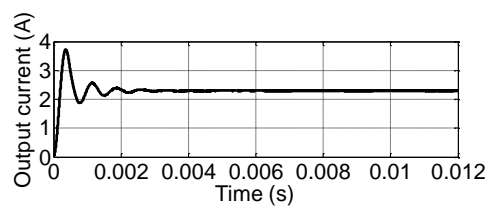


Figure 10. Output current waveform of the IBC

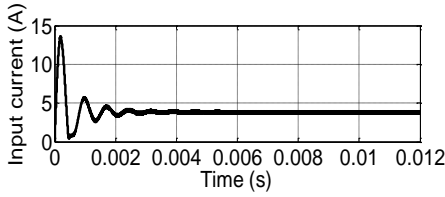


Figure 11. Input current waveform of the IBC

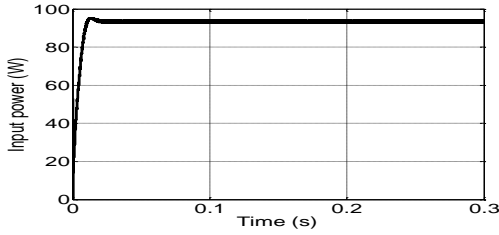


Figure 12. Input power to IBC from PV panel

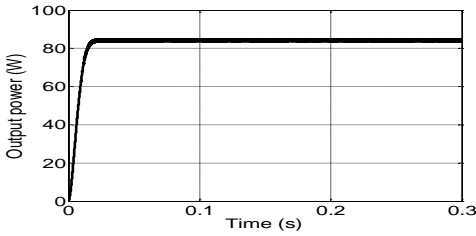


Figure 13. Output power from the IBC

4. 3. Steady State Ripple Waveforms of IBC

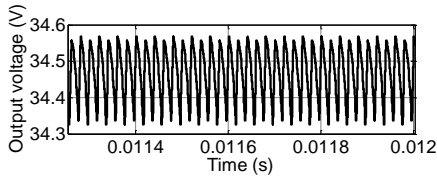


Figure 14. Output voltage ripple waveform of the IBC

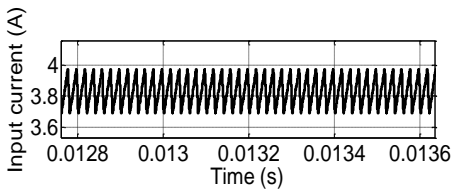


Figure 15. Input current ripple waveform of the IBC

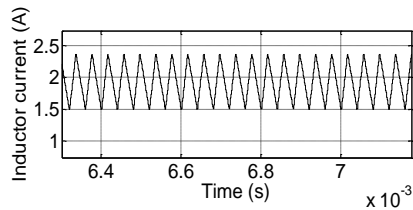


Figure 16. Inductor current ripple waveform of the IBC

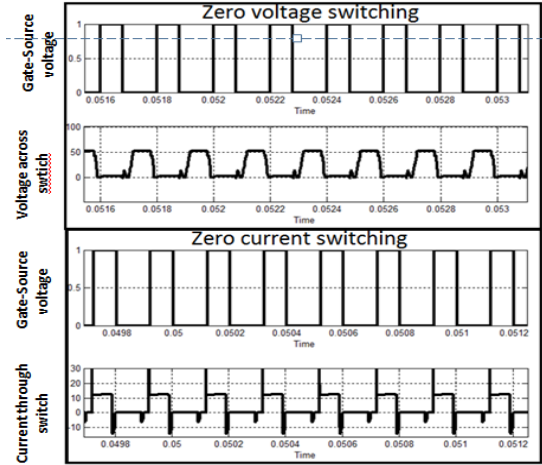


Figure 17. ZVS and ZCS waveforms for IBC

TABLE 3. Ripple calculation

Parameter	Soft switched IBC	Conventional IBC
Output voltage ripple	0.144V	2.33V
Input current ripple	0.0779A	1.234A
Inductor current ripple	0.4416A	0.845 A

4. 4. Calculation of Ripple Value

The ripple values are calculated from the simulation. Waveforms and its comparison with conventional IBC are shown in Table 3. From Table 3, it is found that, the proposed soft-switched IBC gives a reduced output voltage and input current ripple compared to the conventional one.

4. 5. Calculation of Losses in Switching Devices

The losses for the proposed IBC [3, 4] is calculated by finding the conduction and switching losses of the switches as discussed below:

• Switching loss

$$P_{sw} = 0.5 * V_{DS} * I_D * f_s * t_{sw}$$

where V_{DS} is the drain to source voltage

I_D is the drain current

f_s is the switching frequency

t_{sw} is the sum of the rise time and fall time

• Conduction loss

$$P_c = I^2 * R_{d(on)} * D$$

where I is the current through the device, $R_{d(on)}$ is the on state resistance.

The switching and conduction losses for both the switches S_{S1} and S_{S2} are as follows:

Switching loss for S_{S1} and S_{S2} : 0.157092W

Conduction loss for S_{S1} and S_{S2} : 1.1859W

Total device losses=Switching losses+Conduction Losses. Total losses for individual switches are as follows:

$$\text{Switch } S_{S1}=0.157092\text{W}+1.1859\text{W}=1.342992\text{W}$$

$$\text{Switch } S_{S2}=0.157092\text{W}+1.1859\text{W}=1.342992\text{W}$$

$$\text{Total losses}=2.685984\text{W}$$

4. 6. Calculation of Efficiency of IBC From Figures 12 and 13, the input power and output power of the IBC are input power, $P_{in}=95.09\text{W}$ and output power, $P_{out}=89.5\text{W}$

$$\text{Efficiency}=P_{out}/P_{in}=(89.5/95.09)*100=94.11\%.$$

5. HARDWARE IMPLEMENTATION

The entire hardware consists of the gate drive, the converter circuit and a PV panel to provide input voltage to the converter. Here the implementation is done without the use of an MPPT algorithm. For the switches, MOSFETs are used and to provide isolation between the drive circuit and the switches, optocouplers are used. The output pulse from the optocoupler is used to trigger the switches.

The output voltage from the PV panel is not a constant one. It keeps varying with temperature and irradiance. So, the converter is not directly fed from the PV panel. Instead, it is used to charge a battery using a charge controller and this output is given to the converter as shown in Figure 18. The charge controller maintains proper charging voltage on the batteries. It also blocks reverse current and also prevents battery overcharge.

Here, a 12V battery is charged from the PV panel using a charge controller. This 12V is fed as input to the IBC circuit. The input voltage fed to the IBC is 11.5V. The duty cycle of operation is 40%. Thus, using the relation $V_{out}=V_{in}/(1-D)$, we can find that, $V_{out}=11.5/(1-0.4)\approx 19.3\text{V}$ which is shown in Figure 19. From the hardware, the losses of the device was found to be 2.978W and the output voltage ripple was 0.144V. Therefore, the proposed IBC is a better topology for PV applications.

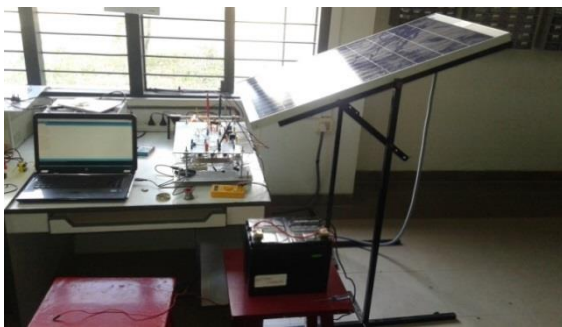


Figure 18. Hardware arrangement of soft switched IBC

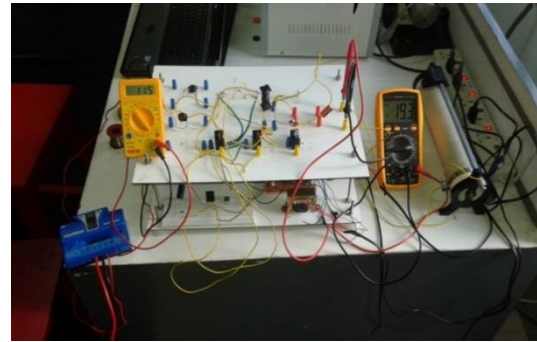


Figure 19. Input and output voltage of the IBC

6. CONCLUSION

This paper provides an insight to the use of soft switching technique for an interleaved boost converter (IBC) for photovoltaic (PV) applications. The primary objective is to reduce switching losses and switching stress on the main switches. This is achieved using ZVS (zero voltage switching) and ZCS (zero current switching) methods operating in lower and higher duty cycles. By using the concept of impedance matching between the resonant tank circuit and output capacitor, the circuit can drive heavy loads with high efficiency. In order to use the converter for photovoltaic applications, it is coupled with a PV panel since solar energy is freely available. Thus by implementing soft switching, the voltage stress on the main switches is reduced, the losses are reduced and also the ripples in the voltage and current waveforms are less. Additionally, the efficiency of the converter is also increased. Hence, the proposed soft switched IBC is an ideal choice for PV applications.

7. ACKNOWLEDGEMENT

The authors wish to thank the Management of SSNCE for funding this research work.

8. REFERENCES

1. Salmi, T., Bouzguenda, M., Gastli, A. and Masmoudi, A., "Matlab/simulink based modeling of photovoltaic cell", *International Journal of Renewable Energy Research (IJRER)*, Vol. 2, No. 2, (2012), 213-218.
2. Selmi, T., Abdul-Niby, M. and Devis, L., "P&o mppt implementation using matlab/simulink", in *Ecological Vehicles and Renewable Energies (EVER)*, Ninth International Conference on, IEEE., (2014), 1-4.
3. Talaat, Y., Hegazy, O., Amin, A. and Lataire, P., "Control and analysis of multiphase interleaved dc/dc boost converter for photovoltaic systems", in *Ecological Vehicles and Renewable Energies (EVER)*, Ninth International Conference on, IEEE., (2014), 1-5.

4. Gu, Y. and Zhang, D., "Interleaved boost converter with ripple cancellation network", *Power Electronics, IEEE Transactions on*, Vol. 28, No. 8, (2013), 3860-3869.
5. Jangwanitlert, A. and Songboonkaew, J., "A comparison of zero-voltage and zero-current switching phase-shifted pwm dc-dc converters", in *Power Electronics and Drives Systems.. PEDS. International Conference on, IEEE. Vol. 1, (2005), 95-100.*
6. Fitzgerald, C. and Duffy, M., "Investigation of coupled inductors in a phase interleaved boost module-integrated-converter", in *Power Electronics for Distributed Generation Systems (PEDG), IEEE 5th International Symposium on, IEEE., (2014), 1-5.*
7. Karimi, R., Adib, E. and Farzanehfard, H., "Resonance based zero-voltage zero-current switching full bridge converter", *Power Electronics, IET*, Vol. 7, No. 7, (2014), 1685-1690.
8. Park, S., Park, Y., Choi, S., Choi, W. and Lee, K.-B., "Soft-switched interleaved boost converters for high step-up and high-power applications", *Power Electronics, IEEE Transactions on*, Vol. 26, No. 10, (2011), 2906-2914.
9. Vijayabhasker, R., Palaniswami, S., Kumar, V.V. and Kumar, M.N.R., "An analysis of interleaved boost converter with lc coupled enhanced soft switching", *American Journal of Applied Sciences*, Vol. 10, No. 4, (2013), 331.
10. Li, W., Deng, Y., Xie, R., Shi, J. and He, X., "Interleaved zvt boost converters with winding-coupled inductors and built-in lc low pass output filter suitable for distributed fuel cell generation system", in *Power Electronics Specialists Conference.. PESC. IEEE, (2007), 697-701.*
11. Zainudin, H.N. and Mekhilef, S., "Comparison study of maximum power point tracker techniques for pv systems", *Proceedings of the 14 th International Middle East Power Systems Conference (MEPCON'10), Cairo University, Egypt, December 19-21, (2010),*

Analysis and Experimentation of Soft Switched Interleaved Boost Converter for Photovoltaic Applications

N. Subramanian, P. Prasanth, R. Srinivasan, R. R. Subhesh, R. Seyerzhai

Department of EEE, SSN College of Engineering, Chennai, India

P A P E R I N F O

چکیده

Paper history:

Received 17 June 2015
Received in revised form 01 July 2015
Accepted 03 September 2015

Keywords:

Soft Switching
Auxiliary Tank
Power Loss Reduction
Photovoltaic

منابع انرژی متداول به سرعت در حال اتمام هستند که این مساله به شیوه های حفاظت ضعیف و استفاده بیش از حد از این منابع مربوط می شود در حالی که تقاضای انرژی در جهان به صورت لحظه ای در حال افزایش است. علاوه بر این، هزینه تولید انرژی متعارف در حال افزایش است که منجر به افزایش آلودگی زیست محیطی می شود. از این رو، لازم است تا نگاهی به منابع انرژی جایگزین مانند خورشید، آب و باد داشت. فتوولتائیک (PV) یک گزینه بسیار امیدبخش است چرا که از انرژی نور خورشید که به طور طبیعی در دسترس است و در سراسر زمین توزیع شده است استفاده می کند که نه تنها آلودگی ندارد بلکه رایگان، فراوان و قابل بازیافت در طبیعت است. از میان مبدل‌های DC-DC مختلف ارائه شده در متون، مبدل بوسست لایه بهترین گزینه برای PV و دیگر کاربردهای چگالی توان بالا است. مبدل های بوسست متداول دچار تلفات سوئیچ و تنشهای سوئیچ در طول دوره روشن و خاموش شدن می شوند که علت آن سوئیچینگ سخت است. به منظور حذف اتلاف توان در دستگاه های مبدل، مبدل‌های IBC در این مقاله ارائه شده است. سوئیچینگ نرم با استفاده از یک مدار مخزن رزونانس LC به دست می آید. مدار مخزن مسئول ولتاژ سوئیچینگ صفر (ZVS) و سوئیچینگ جریان صفر (ZCS) است، که به میزان زیادی موجب حذف اتلاف توان در سوئیچ می شود. از آنجا که منبع فتوولتائیک به عنوان ورودی به مبدل استفاده می شود، الگوریتم MPPT برای استخراج حداکثر توان در دسترس از پانل PV استفاده شده است. علاوه بر این، اتلاف دستگاه، موج دار شدن و به اشتراک گذاری جریان بر اساس ویژگی های ورودی و خروجی ثبت و مورد بررسی قرار می گیرد. مطالعه شبیه سازی از طرح با استفاده از نرم افزار MATLAB / SIMULINK software انجام می شود. نمونه سخت افزار با ماژول PV برای ارزیابی نتایج شبیه سازی توسعه داده شده است.

doi: 10.5829/idosi.ije.2015.28.10a.10